Electron capture in quantum wells via scattering by electrons, holes, and optical phonons

Karol Kálna and Martin Moško
Institute of Electrical Engineering, Slovak Academy of Sciences, Dúbravská cesta 9, Sk-842 39 Bratislava, Slovakia
(Received 3 June 1996; revised manuscript received 7 August 1996)

Electron-capture times due to the electron-electron (e-e), electron-hole (e-h), and electron-polar optical phonon (e-pop) interactions are calculated in the GaAs quantum well (QW) with electron and hole densities 10^{11} cm^{-2}. The calculated capture times oscillate as a function of the QW width with the same period but with different amplitudes. The e-h capture time is two to four orders larger and the e-e capture time one to three orders larger than the e-pop capture time. The exceptions are the QW widths near resonance minima, where the e-e capture time is only $2-3$ times larger and the e-h capture time $10-100$ times larger. A different physical origin of the oscillatory behavior is demonstrated for the e-e and e-pop capture times. Effects of exchange and degeneracy on the e-e capture are analyzed. The exchange effect increases the e-e capture time approximately two times while the degeneracy does not change the capture time except for the QW depths and widths near the resonance. [S0163-1829(96)01948-6]

I. INTRODUCTION

Electron capture represents the transition of an electron from the state above the barrier into a bound state in the quantum well (QW). In a QW laser the electrons and holes captured in the QW can create population inversion and participate through mutual recombination in the laser action. Therefore, the shorter the capture time, the faster the creation of population inversion, and the laser works at a lower threshold current and/or with a better high-speed modulation characteristics.

Since in QW lasers the wavelengths of captured electrons are comparable with the QW width and their coherence length exceeds the barrier width,[1] the classical diffusive models[2,3] have to be replaced by quantum-mechanical (QM) ones. Previous QM calculations predicted that the polar optical phonon (pop) emission induced capture time in the single QW oscillates[4,5] in dependence on the QW width. These oscillations were observed in the separate confinement heterostructure quantum well (SCHQW),[6] in the multiple-quantum-well structure,[7] and in the QW structure with tunnel barriers.[8]

The electron and hole capture processes are expected to play an important role in the optimization of QW laser performance. The hole capture is faster due to the large hole effective mass and studies of the capture are therefore focused mainly on electrons.[9–11] The difference between the electron and hole capture times tends to diminish during the capture process[12] due to an electron-hole attraction and due to the ambipolar character of the capture. Minimization of the electron capture time can be achieved mainly by optimizing the QW width and depth. While the capture due to the electron-polar optical phonon (e-pop) interaction is dominant outside the oscillation minima, in the minima the electron-electron (e-e) interaction can play an important role[9] and becomes dominant for high enough electron densities. Increasing influence of the e-e capture with increasing electron density in the QW was confirmed in Refs. 13 and 14 where the electron degeneracy and the dynamic screening function in a coupled system of electrons and phonons were taken into account. Similarly to Ref. 9 the exchange effect was not considered.

The exchange effect was previously included in the carrier-carrier (c-c) thermalization of photoexcited spin-polarized two-dimensional (2D) carriers in the lowest energy level of the GaAs QW.[15,16] In this case the inclusion of the exchange slows down the thermalization many times. Recently, the exchange has been incorporated into the intersubband c-c scattering rate in the GaAs QW.[17]

In this work we wish to extend our previous calculations of the e-e interaction induced capture time[9] by taking into account the exchange.[17] We consider also the electron capture due to the electron-hole (e-h) interaction where besides the electron screening also the screening by the holes (often neglected in similar analyzes) is incorporated into the static screening function. Finally, we analyze different physical origins of the oscillatory behavior of the e-e and e-pop capture times.

The e-h interaction-induced capture time in the SCHQW oscillates with the same period as the e-e and e-pop capture times but with a larger oscillation amplitude than the amplitude of the e-e capture time. The e-h capture time is even larger in the oscillation minima. The degeneracy influences the value of the e-e capture time only in the resonance. The exchange effect increases its value two times outside the resonance and about 10% in the resonance.

In Sec. II the e-h, e-e, and e-pop scattering rates are described including the effects of the exchange and degeneracy in the e-e interaction. The calculated electron capture times are discussed in Sec. III and the results are summarized in Sec. IV.

II. CARRIER-CARRIER SCATTERING RATE

Figure 1 shows the band edge profile of the SCHQW structure analyzed in this work. The structure consists of the $Al_xGa_{1-x}As/GaAs/Al_xGa_{1-x}As$ QW with 500-Å $Al_xGa_{1-x}As$ barriers, embedded between two semiinfinite AlAs layers.[1,11] The AlAs barrier V_b is 1.07 eV. To have the $Al_xGa_{1-x}As$ barrier V_w equal to 0.3 eV we take the alu-

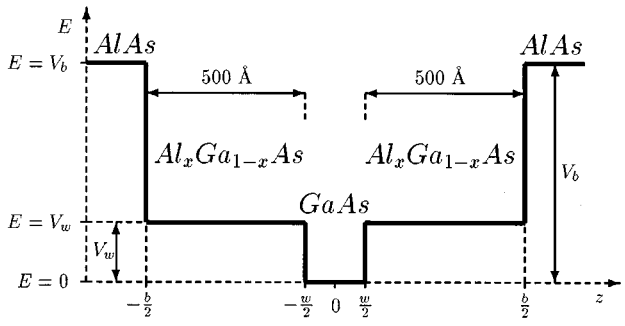

FIG. 1. Conduction-band edge diagram (schematic) and geometry of the separate confinement heterostructure quantum well considered in our calculations.

minium content $x=0.305$.[18] The carrier density in the QW is $N_S=10^{11}$–10^{12} cm^{-2} and the lattice temperature is 8 K. The same structure has been considered in previous analyzes,[1,6,9,11] since it is of some interest for optical measurements of the capture time as well as for laser applications.

The c-c scattering rate in the structure is treated in the Born approximation according to Ref. 17. Let the carrier α occupy the subband i with wave vector $\mathbf{k}_1$ and the carrier β occupy the subband j with wave vector $\mathbf{k}_2$. Due to a mutual Coulomb interaction the carrier α is scattered into the subband m with wave vector $\mathbf{k}_1'$ and the partner carrier β is scattered into the subband n with wave vector $\mathbf{k}_2'$. The c-c scattering rate of a carrier with wave vector $\mathbf{k}_1$ from the subband i to the subband j can be obtained as

$$\lambda_{im}^{\alpha\beta}(\mathbf{k}_1)=\frac{1}{N_S A}\sum_{j,n,\mathbf{k}_2} f_j^{\beta}(\mathbf{k}_2)\lambda_{ijmn}^{\alpha\beta}(g), \quad \alpha,\beta=e,h, \quad (1)$$

where $g=|\mathbf{k}_1-\mathbf{k}_2|$. The summation over $\mathbf{k}_2$ is assumed to include both spin orientations, the summation over j,n involves the subbands below the $Al_xGa_{1-x}As$ barrier. A is the normalization area, $f_j^{\beta}(\mathbf{k}_2)$ is the Fermi distribution function of the carriers β in the subband j, and $\lambda_{ijmn}^{\alpha\beta}(g)$ is the c-c pair scattering rate.

The electron capture time is reciprocal of the electron capture rate,

$$\tau_{e-\eta}^{-1}=\frac{\sum_{i,m,\mathbf{k}_1} f_i^e(\mathbf{k}_1)\lambda_{im}^{e\eta}(\mathbf{k}_1)}{\sum_{i,\mathbf{k}_1} f_i^e(\mathbf{k}_1)}, \quad \eta=e,h, \quad (2)$$

where the summation over i (m) includes only the subbands above (below) the $Al_xGa_{1-x}As$ barrier and $f_i^e(\mathbf{k}_1)$ is the electron distribution in the subband i.

A. Electron-hole pair scattering rate

The e-h pair scattering rate is calculated considering the screening by electrons and holes occupying the lowest-energy subband (see the Appendix). It reads

$$\lambda_{ijmn}^{eh}(g)=\frac{N_S m_r e^4}{16\pi\hbar^3\kappa^2}\int_0^{2\pi} d\theta \times\left[F_{ijmn}^{eh}(q)-\frac{q_s^e}{q\epsilon^{eh}(q)}F_{i1m1}^{ee}(q)G_{1j1n}(q)+\frac{q_s^h}{q\epsilon^{eh}(q)}F_{i1m1}^{eh}(q)H_{1j1n}(q)\right]^2 q^{-2}, \quad (3)$$

where the e-h static screening function $\epsilon^{eh}(q)$ is given by

$$\epsilon^{eh}(q)=\left(1+\frac{q_s^e}{q}F_{1111}^{ee}(q)\right)\left(1+\frac{q_s^h}{q}F_{1111}^{hh}(q)\right)-\frac{q_s^e}{q}F_{1111}^{eh}(q)\frac{q_s^h}{q}F_{1111}^{he}(q), \quad (4)$$

$$G_{1j1n}(q)=F_{1j1n}^{eh}(q)\left[1+\frac{q_s^h}{q}F_{1111}^{hh}(q)\right]-\frac{q_s^h}{q}F_{1j1n}^{hh}(q)F_{1111}^{he}(q),$$

$$H_{1j1n}(q)=F_{1j1n}^{hh}(q)\left[1+\frac{q_s^e}{q}F_{1111}^{ee}(q)\right]-\frac{q_s^e}{q}F_{1j1n}^{eh}(q)F_{1111}^{eh}(q),$$

$$q=\frac{1}{2}\left[2g^2+\frac{4m_r}{\hbar^2}E_S^{eh}-2g\left(g^2+\frac{4m_r}{\hbar^2}E_S^{eh}\right)^{1/2}\cos\theta\right]^{1/2}, \quad (5)$$

and $E_S^{eh}=E_i^e+E_j^h-E_m^e-E_n^h$. In the above formulas the reduced effective mass $m_r=2m_e m_h/(m_e+m_h)$, the relative vector $\mathbf{g}=m_r(\mathbf{k}_2/m_h-\mathbf{k}_1/m_e)$, κ is the static permittivity, the electron and hole effective masses are denoted as m_e and m_h, and the electron and hole subband energies as $E_\gamma^e(\gamma=i,m)$ and $E_\delta^h(\delta=j,n)$, respectively. Finally, $q_s^e=e^2m_e/(2\pi\kappa\hbar^2)f_1^e(\mathbf{k}_2=0)$ and $q_s^h=e^2m_h/(2\pi\kappa\hbar^2)f_1^h(\mathbf{k}_2=0)$.

The form factors in Eq. (3) are defined as

$$F_{ijmn}^{\alpha\beta}(q)=\int_{-\infty}^{\infty}dz_1\int_{-\infty}^{\infty}dz_2\chi_i^{\alpha}(z_1)\chi_j^{\beta}(z_2)\times e^{-q|z_1-z_2|}\chi_m^{\alpha}(z_1)\chi_n^{\beta}(z_2), \quad \alpha,\beta=e,h, \quad (6)$$

where the wave function χ_γ^α of the carrier α in the subband $\gamma(\gamma=i,j,m,n)$ is obtained assuming the x-dependent carrier effective mass and the flat Γ band with parabolic energy dispersion, both properly interpolated between GaAs and AlAs.[18]

B. Electron-electron pair scattering rate

The e-e pair scattering rate is found in a similar way (see the Appendix) as the e-h pair scattering rate. Taking into account only the screening by electrons in the lowest subband, one gets

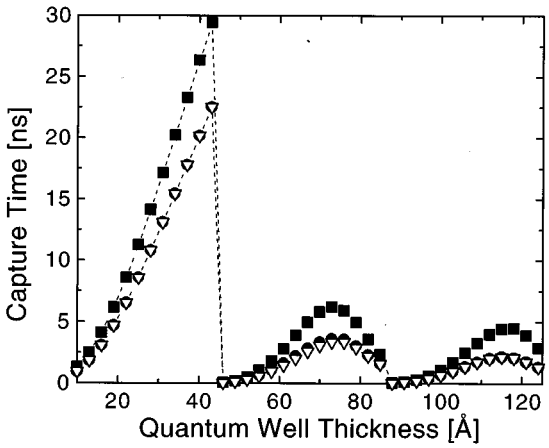

FIG. 2. e-e capture time as a function of QW width for various static screening models. The capture time calculated using the e-e scattering rate (7) (open triangles) is compared with the capture times calculated using the e-e scattering rate (12) screened by the screening function (8) with realistic $F_{1111}(q)$ (full circles) and with $F_{1111}(q)=1$ (full squares).

$$\lambda^{ee}_{ijmn}(g)=\frac{N_S m_e e^4}{16\pi\hbar^3\kappa^2}\int_0^{2\pi} d\theta \times\left[F^{ee}_{ijmn}(q)-\frac{q^e_s}{q\epsilon^e(q)}F^{ee}_{i1m1}(q)F^{ee}_{1j1n}(q)\right]^2 q^{-2}, \tag{7}$$

where the static screening function $\epsilon^e(q)$ reads

$$\epsilon^e(q)=1+(q^e_S/q)F^{ee}_{1111}(q)f^e_1(\mathbf{k}_1=0), \tag{8}$$

$$q=\frac{1}{2}\left[2g^2+\frac{4m_e}{\hbar^2}E^e_S-2g\left(g^2+\frac{4m_e}{\hbar^2}E^e_S\right)^{1/2}\cos\theta\right]^{1/2}, \tag{9}$$

and $E^e_S=E^e_i+E^e_j-E^e_m-E^e_n$. In Eq. (8) the static screening by the holes is omitted assuming that the holes are too slow (due to their large effective masses) to follow the fast changes of electron positions.[15] This is a so-called quasidynamic screening model.

It is worth mentioning that the screening [i.e., the term containing the screening function $\epsilon^e(q)$] disappears in Eq. (7) for those transitions in which $F^{ee}_{i1m1}(q)=0$ and/or $F^{ee}_{1j1n}(q)=0$. This happens when $\chi^e_i(z_1)$ is symmetric (antisymmetric) and $\chi^e_m(z_1)$ is antisymmetric (symmetric), and/or when the same holds for $\chi^e_j(z_2)$ and $\chi^e_n(z_2)$.

For example, when the QW contains two energy subbands, the screening effect disappears for the transitions $i,1\rightarrow 1,2$ $(i=3,5,\ldots)$. Then the e-e pair scattering rate reads

$$\lambda^{ee}_{i112}(g)=\frac{N_S m_e e^4}{16\pi\hbar^3\kappa^2}\int_0^{2\pi} d\theta\frac{[F^{ee}_{i112}(q)]^2}{q^2}. \tag{10}$$

Note that the same effect appears also in the e-h pair scattering rate (3).

After simple manipulations, the integrand in Eq. (7) can be simplified assuming

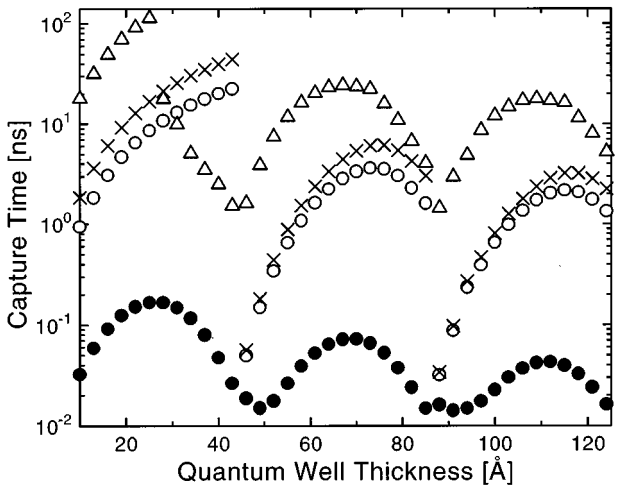

FIG. 3. Electron capture time vs the QW width for the e-pop interaction (full circles), the e-h interaction (open triangles), the e-e interaction without exchange effect (open circles), and the e-e interaction with exchange effect (crosses).

$$\frac{F^{ee}_{ijmn}(q)F^{ee}_{1111}(q)}{F^{ee}_{i1m1}(q)F^{ee}_{1j1n}(q)}\approx 1 \tag{11}$$

into the form[17]

$$\lambda^{ee}_{ijmn}(g)=\frac{N_S m_e e^4}{16\pi\hbar^3\kappa^2}\int_0^{2\pi} d\theta\frac{|F^{ee}_{ijmn}(q)|^2}{q^2\epsilon^e(q)^2}. \tag{12}$$

To justify the approximation (11), the e-e capture times calculated for various screening functions are compared in Fig. 2. In this calculation the electron distribution function $f^e_i(\mathbf{k}_1)$ in the formula (2) was taken as a constant distribution up to the pop energy above the $Al_xGa_{1-x}As$ barrier, which roughly models the injected barrier distribution after a rapid phonon cooling.[5] The capture time obtained from the pair scattering rate (12) with the screening function (8) is almost the same as the capture time obtained from the pair scattering rate (7). If (following Ref. 19) we use Eq. (12) with $F^{ee}_{1111}(q)=1$ in the screening function (8), the calculated capture time overestimates both capture times more than by 20%.

C. Electron-electron pair scattering rate with degeneracy and exchange

To include the Pauli exclusion principle in the e-e scattering rate Eq. (7) we can start from the equation

$$\lambda^{ee}_{ijmn}(g)=\frac{N_S m_e e^4}{8\pi\hbar^3\kappa^2}\int d\mathbf{k}'_2[1-f^e_m(\mathbf{k}_1+\mathbf{k}_2-\mathbf{k}'_2)] \times[1-f^e_n(\mathbf{k}'_2)]\frac{[F^{ee}_{ijmn}(q_l)]^2}{q_l^2\epsilon^e(q_l)^2} \times\delta\left(\frac{\hbar^2}{2m_e}(\mathbf{k}_1^2+\mathbf{k}_2^2-\mathbf{k}_1'^2-\mathbf{k}_2'^2)+E^e_S\right), \tag{13}$$

in which $\mathbf{k}_1'=\mathbf{k}_1+\mathbf{k}_2-\mathbf{k}_2'$. The δ function simplifies the integration over $\mathbf{k}_2'$ in Eq. (13) and then the *e*-*e* pair scattering rate with degeneracy is given by

$$\lambda_{ijmn}^{ee}(g)=\frac{N_S m_e e^4}{8\pi\hbar^3\kappa^2}\sum_{l=1}^{2}\int_0^{2\pi}d\theta\frac{p_l}{|D-2p_l|}[1-f_m^e(r_l)]\times[1-f_n^e(p_l)]\frac{[F_{ijmn}^{ee}(q_l)]^2}{q_l^2\epsilon^e(q_l)^2},\tag{14}$$

where

$$q_l=[p_l{}^2+k_2^2-2k_2p_l\cos(\theta-\phi)]^{1/2},\quad l=1,2$$

$$r_l=[k_1^2+k_2^2+p_l-2k_1k_2\cos\phi-2k_1p_l\cos\theta+2k_2p_l\cos(\theta-\phi)]^{1/2},$$

$$p_1=\frac{1}{2}D+\frac{1}{2}\left[D^2+\frac{4m}{\hbar^2}E_S^e-4k_1k_2\cos\phi\right]^{1/2},$$

$$p_2=\frac{1}{2}D-\frac{1}{2}\left[D^2+\frac{4m}{\hbar^2}E_S^e-4k_1k_2\cos\phi\right]^{1/2},$$

$$D=k_1\cos\theta+k_2\cos(\theta-\phi).$$

The angles θ and ϕ in the above expressions are between the wave vectors $\mathbf{k}_1,\mathbf{k}_2'$ and $\mathbf{k}_1,\mathbf{k}_2$, respectively.

Electrons are indistinguishable particles. Therefore, the scattering rate (7) should include the exchange effect.[15] According to Ref. 17 the exchange can be incorporated into the intersubband *e*-*e* scattering rate (14) using the replacement

$$\frac{|F_{ijmn}^{ee}(q_l)|^2}{q_l^2\epsilon^e(q_l)^2}\mapsto\frac{1}{2}\left[\frac{|F_{ijmn}^{ee}(q_l)|^2}{q_l^2\epsilon^e(q_l)^2}+\frac{|F_{ijnm}^{ee}(q_l')|^2}{q_l'^2\epsilon^e(q_l')^2}-\frac{F_{ijmn}^{ee}(q_l)F_{ijnm}^{ee}(q_l')}{q_l\epsilon^e(q_l)q_l'\epsilon^e(q_l')}\right],\tag{15}$$

where

$$q_l'=[p_l{}^2+k_1^2-2k_1p_l\cos(\theta)]^{1/2},\quad l=1,2.$$

D. Electron-polar optical phonon scattering rate

The *e*-pop scattering rate of an electron with wave vector $\mathbf{k}_1$ from subband i to subband m for a spontaneous phonon emission only reads[20,21]

$$\lambda_{im}^{e\text{-pop}}(\mathbf{k}_1)=\frac{e^2\omega m_e}{8\pi\hbar^2}\left(\frac{1}{\kappa_\infty}-\frac{1}{\kappa}\right)\int_0^{2\pi}d\theta\frac{F_{iimm}^{ee}(q)}{q\epsilon^e(q)},\tag{16}$$

$$q=\left[2k_1^2+\frac{2m_e}{\hbar^2}E_S^P-2k_1\left(k_1^2+\frac{2m_e}{\hbar^2}E_S^P\right)^{1/2}\cos\theta\right]^{1/2},\tag{17}$$

where $E_S^P=E_i-E_m-\hbar\omega$, $\hbar\omega$ is the pop energy and κ_∞ is the high-frequency permittivity. To obtain the *e*-pop capture time the same formula as Eq. (2) can be used after replacing η by pop.

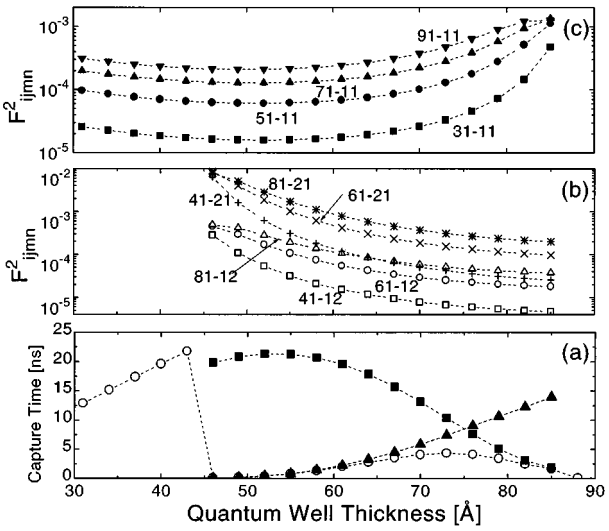

FIG. 4. (a) *e*-*e* capture time vs the QW width. The total capture time from Fig. 3 (open circles) is split into the *e*-*e* capture time to state 1,1 (full squares) and into the *e*-*e* capture time to states 1,2 and 2,1 (full triangles). (b) Squares of the *e*-*e* form factors F_{i112} and F_{i121} vs the QW width for $q=3\times10^8$ m^{-1}. (c) Squares of the *e*-*e* form factors F_{i111} vs the QW width for $q=3\times10^8$ m^{-1}.

III. ELECTRON CAPTURE TIMES

Figure 3 shows the electron capture time versus the QW width for *e*-*e*, *e*-*h*, and *e*-pop interactions where, in the case of the *e*-*e* interaction, the results obtained with and without the exchange effect are distinguished. In these calculations the function $f_i^e(\mathbf{k}_1)$ in formula (2) is taken as a constant distribution up to the pop energy above the $Al_xGa_{1-x}As$ barrier. The capture times oscillate with the QW width and reach the minimum whenever a new bound state merges into the QW.[9] At small QW widths, when the QW contains only one bound state, the *e*-*h* and *e*-*e* capture times increase with an increasing QW width. At the QW widths at which the second bound state merges into the QW ($\sim$30 Å for holes, 46 Å for electrons), the *e*-*h* and *e*-*e* capture times decrease suddenly by several orders of magnitude. With a further increase of the QW width the oscillatory behavior persists, but the oscillations become smooth. To understand this feature we split in Fig. 4(a) the total *e*-*e* capture time from Fig. 3 into the *e*-*e* capture time to states 1,1 (full squares) and the *e*-*e* capture time to states 1,2 and 2,1 (full triangles). A smooth decrease of the total capture time from its maximum value at $w=73$ Å is due to the decrease of the capture time to states 1,1 with w. This decrease is caused by the increase of relevant form factors [Fig. 4(c)] with w. At the same time the capture time to state 1,2 and 2,1 increases with w due to the decrease of relevant form factors [Fig. 4(b)] with w.

The behavior of the *e*-pop capture time is quite different. The decrease of the *e*-pop capture time to its oscillation minima is smooth even when the first minimum appears. The *e*-pop capture time curve does not show a resonant drop for the QW widths near the resonances, because the barrier electrons occupy the states below the threshold for the pop emission and cannot be scattered into the subband, which is in resonance with the top of the QW. A further increase of the QW width shifts the resonant subband deeper into the QW

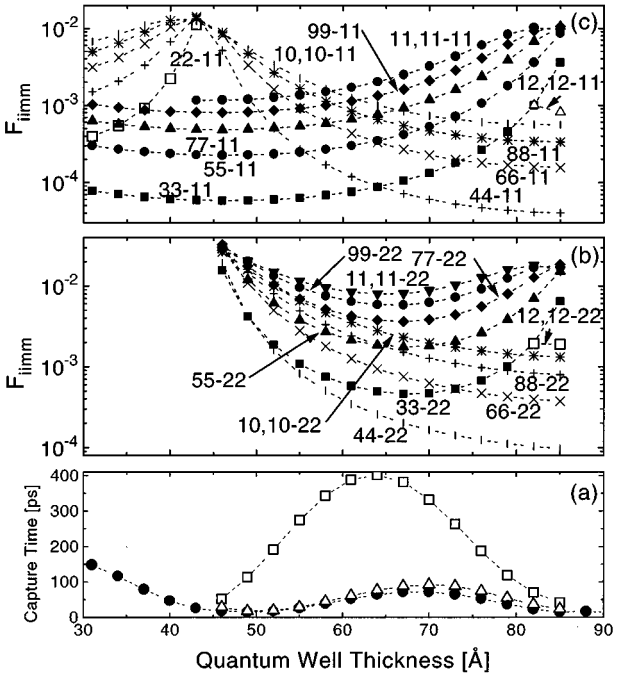

FIG. 5. (a) e-pop capture time vs the QW width. The total capture time from Fig. 3 (full circles) is split into the e-pop capture time to state 1,1 (open squares) and into the e-pop capture time to state 2,2 (open triangles). (b) The e-pop form factors F_{ii22} vs the QW width for $q=3\times10^8$ m^{-1}. (c) The e-pop form factors F_{ii11} vs the QW width for $q=3\times10^8$ m^{-1}.

and the e-pop scattering into this subband smoothly increases. The exception is a monoenergetic distribution with the energy close to the pop energy. In such case the e-pop scattering into the resonance subband is not prohibited and a resonant decrease of the e-pop capture time takes place.[14] Similarly to the e-e interaction case we split in Fig. 5(a) the total e-pop capture time from Fig. 3 into the e-pop capture time to states 1,1 (open squares) and the e-pop capture time to states 2,2 (open triangles). Transitions to the highest subband in the QW play always a more important role than transitions to the lower subbands. This fact explains the behavior of the relevant form factors in dependence on the QW width in Figs. 5(b) and 5(c).

The total electron capture time that is, in fact, measured in an experiment can be obtained as

$$\tau_{e\text{-tot}}=\frac{\tau_{e\text{-}e}\tau_{e\text{-pop}}}{\tau_{e\text{-}e}+\tau_{e\text{-pop}}}. \tag{18}$$

In Fig. 6 the e-pop capture time (full circles) is compared with the total electron capture times (open symbols) obtained using the e-e capture time with exchange for the electron density $N_S=10^{11}$ and 10^{12} cm^{-2}. This figure depicts how the e-e interaction affects the total electron capture time near the resonance and how its effect decreases the total electron capture time when the electron density is higher. A direct comparison of our total electron capture time with the experiments[6–8] is not possible because we use the step distribution function for an active laser regime. Nevertheless, we have obtained the resonances in the capture time oscillations by the same QW width as resonances measured in the experiments. The direct comparison requires one to take into account the ambipolar capture time, which can only be calculated when the hole capture time is fitted to the experimental data.[6,12]

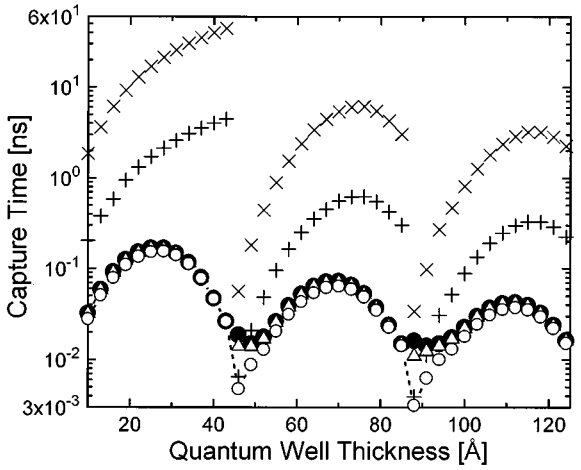

FIG. 6. Total electron capture times vs the QW width for the electron density 10^{11} cm^{-2} (open triangles) and for the electron density 10^{12} cm^{-2} (open circles) are compared with the e-pop capture time (full circles). Electron capture times for the e-e interaction with exchange effect are also shown for the electron density 10^{11} cm^{-2} (crosses) and 10^{12} cm^{-2} (plusses).

To directly detect the e-e capture time it is necessary to suppress the e-pop interaction. A proper structure for the e-pop interaction suppression is the structure with the QW depth smaller than the pop energy. If in the time-resolved

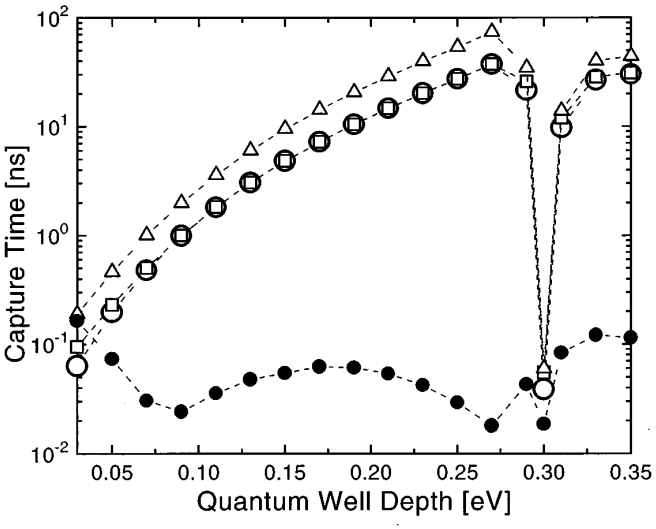

FIG. 7. Electron capture time as a function of QW depth for the QW width of 46 Å. Open circles are for the e-e interaction without degeneracy and exchange effect, open squares are for the e-e interaction with degeneracy, open triangles are for the e-e interaction with degeneracy and exchange effect, and full circles are for the e-pop interaction-induced capture time. In the calculations the distribution function $f_i^e(\mathbf{k}_1)$ in the capture time formula (2) is the Boltzmann distribution at the electron temperature 70 K.

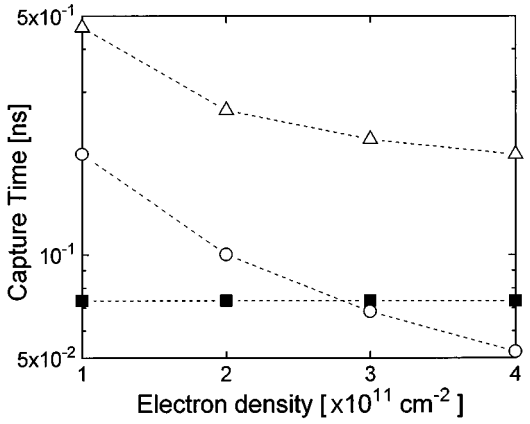

FIG. 8. Electron capture time vs the electron density for the QW with $V_w = 0.05$ eV and $w = 46$ Å. Open circles (triangles) represent the capture time for the e-e interaction without (with) degeneracy and exchange effect, respectively, and full squares represent the capture time for the e-pop interaction.

optical experiment[6] such structure would be irradiated by a short laser pulse, the excited carriers above the barrier would thermalize to the Boltzmann distribution with the electron temperature T_e during several picoseconds[6,22] and after that they would be captured via the e-e interaction into the QW. Figure 7 shows the electron capture time versus the QW depth for the QW width equal to 46 Å. Here we assume that the QW depth varies with the aluminum content x according to the relation $V_w = (0.9456x + 0.1288x^2)$ eV.[18] In this calculation the distribution function $f_i^e(\mathbf{k}_1)$ in the capture time formula (2) is taken as the Boltzmann distribution function at the electron temperature $T_e = 70$ K. This choice corresponds to the assumption that the electrons are optically excited only a few meV above the $Al_xGa_{1-x}As$ barrier. Figure 7 also shows that the e-e capture dominates if the QW depth is less than 0.04 eV. The degeneracy and exchange affect the e-e capture time substantially at a small QW depth.

The electron capture times from Fig. 8 illustrate the inclusion and exclusion of the degeneracy and exchange effect in the e-e interaction with an increasing electron density for the shallow QW ($V_w = 0.05$ eV, $w = 46$ Å). In such structures, recently also considered in Ref. 23, the e-e capture time is of similar importance as the e-pop capture time for higher electron densities although it was calculated including the degeneracy and exchange effect in the e-e interaction, which increases the capture time by about two times.

Outside the resonance the exchange increases the e-e capture time by about two times due to the following reasons. In the case where both electrons are scattered into the same subband ($m = n$), all three terms in the substitution (15) have almost the same magnitude (which we verify numerically) because the values of q and q' are very close. In the case where both electrons are scattered into different subbands ($m \neq n$), it is necessary to take into account that the substitution (15) is summed in formulas (1) and (2) over the final states m and n. In the sum the terms with final states m,n and n,m can be rewritten as

$$\frac{1}{2}\left[\frac{|F_{ijmn}(q)|^2}{q^2\epsilon(q)^2} + \frac{|F_{ijnm}(q)|^2}{q^2\epsilon(q)^2}\right] + \frac{1}{2}\left[\frac{|F_{ijnm}(q')|^2}{q'^2\epsilon(q')^2} + \frac{|F_{ijmn}(q')|^2}{q'^2\epsilon(q')^2}\right] - \frac{1}{2}\left[\frac{F_{ijmn}(q)F_{ijnm}(q')}{q\epsilon(q)q'\epsilon(q')} + \frac{F_{ijnm}(q)F_{ijmn}(q')}{q\epsilon(q)q'\epsilon(q')}\right]. \quad (19)$$

All three terms in Eq. (19) have almost the same magnitude, which we verify numerically. Consequently, the presence of the third (interference) term decreases the value of the expression (19) two times in comparison with the case when the exchange effect (i.e., the interference term) is neglected. Finally, in the resonance the exchange increases the capture time by only 10%. This is due to the fact that in the resonance the values of q and q' strongly differ and the interference term becomes much smaller than direct terms.

The effect of degeneracy on the capture time is negligible when the difference between the lowest-energy subband above the barrier and the highest-energy subband in the QW is large compared to the quasi-Fermi energy of the electrons in the QW. In such a case most of the final states in the QW are unoccupied and the e-e capture times with and without degeneracy are quite close. Near the resonance, when the highest-energy subband in the QW is close to the lowest subband above the barrier, the degeneracy strongly reduces the number of available final states despite the fact that the highest subband is essentially unoccupied. This is due to the fact that the electron captured in the highest subband of the QW can exchange only a small amount of energy with the scattering partner in the lowest subband of the QW. The available final states of the scattering partner are therefore blocked by the 8-K Fermi distribution in the QW.

IV. CONCLUSIONS

The e-h, e-e, and e-pop capture times have been calculated in the SCHQW for carrier densites of 10^{11} and 10^{12} cm^{-2}. All three capture times oscillate as a function of the QW width with the same period but with very different amplitudes. The e-h capture time is not only much greater than the e-pop capture time but also greater than the e-e capture time even for the QW widths near the resonance. In the resonance the e-e interaction plays a role together with the e-pop interaction and improves the capture efficiency of the QW.[9] Since the increase of the electron density decreases the e-e capture time, it is expected that the e-h capture time will decrease similarly. Therefore, the influence of the e-h interaction should be considered only for high density and in resonances.

We find that the electron capture time oscillates as a function of the depth and reaches the oscillation minimum when a new bound state merges into the QW. At the same time the effect of the degeneracy and exchange effect on the e-e capture time have been studied. The degeneracy increases the capture time approximately 50% only in the resonant minima. The inclusion of the exchange effect into the e-e

interaction increases the e-e capture time by about two times. To illustrate the quantitative importance of the exchange effect found in this paper, we mention that the quantitative changes due to the dynamic screening and coupling between electrons and phonons (not considered in this work) are much smaller.[13] Therefore, the exchange effect should be considered in the e-e interaction-induced capture.

ACKNOWLEDGMENTS

Numerous useful discussions with A. Mošková are greatly appreciated. We also thank her and B. Olejníková for a careful reading of the manuscript. This work was supported by the Slovak Grant Agency for Science under Contract No. 2/1092/96.

APPENDIX: CARRIER-CARRIER INTERACTION WITH MULTISUBBAND STATIC SCREENING

The statically screened intercarrier interaction in the multisubband 2D system, $V(\mathbf{Q},z_1,z_2)$, can be obtained by solving the integral Poisson equation[21,24]

$$\begin{aligned}V(\mathbf{Q},z_1,z_2)=&\frac{e}{2\kappa Q}e^{-Q|z_1-z_2|}\\&-\sum_{l=1}^{L}\frac{Q_l^e}{Q}\int_{-\infty}^{\infty}dz''[\phi_l^e(z'')]^2e^{-Q|z_1-z''|}\\&\times\int_{-\infty}^{\infty}dz'[\phi_l^e(z')]^2V(\mathbf{Q},z',z_2)\\&-\sum_{k=1}^{K}\frac{Q_k^h}{Q}\int_{-\infty}^{\infty}dz''[\phi_l^h(z'')]^2e^{-Q|z_1-z''|}\\&\times\int_{-\infty}^{\infty}dz'(\phi_l^h(z'))^2V(\mathbf{Q},z',z_2),\end{aligned}\tag{A1}$$

where $L(K)$ is the number of electron (hole) subbands, the first term on the right-hand side is the bar Coulomb interaction, the second and third terms describe the screening by electrons and holes, respectively, and

$$Q_l^e=\frac{e^2m_e}{2\pi\kappa\hbar^2}f_l^e(\mathbf{k}=0),\quad Q_k^h=\frac{e^2m_h}{2\pi\kappa\hbar^2}f_k^h(\mathbf{k}=0)$$

are the 2D electron and 2D hole screening constants in the lth electron and kth hole subband, respectively.

If the Coulomb potential (A1) is multiplied by the electron wave function ϕ_l^e for $l=1,2,\ldots,L$ and by the hole wave function ϕ_k^h for $k=1,2,\ldots,K$, and then integrated over z', the following two sets of mutually coupled equations are found:

$$\begin{aligned}&(1+A_{pp}^e)x_p^e+\sum_{l=1,\ l\neq p}^{L}C_{pl}^{ee}x_l^e+\sum_{k=1}^{K}C_{pk}^{he}x_k^h=B_p^e,\\&\qquad p=1,2,\ldots,L,\\&\sum_{l=1}^{L}C_{rl}^{eh}x_l^e+(1+A_{rr}^h)x_r^h+\sum_{k=1,k\neq r}^{K}C_{rk}^{hh}x_k^h=B_r^h,\\&\qquad r=1,2,\ldots,K,\end{aligned}\tag{A2}$$

where

$$x_i^\eta=\int_{-\infty}^{\infty}dz'[\phi_i^\eta(z')]^2V(Q,z',z_2),$$

$$A_{ii}^\eta=\frac{Q_i^\eta}{Q}\int_{-\infty}^{\infty}dz'[\phi_i^\eta(z')]^2\int_{-\infty}^{\infty}dz''[\phi_i^\eta(z'')]^2e^{-Q|z'-z''|},$$

$$B_i^\eta=\frac{e}{2\kappa Q}\int_{-\infty}^{\infty}dz'[\phi_i^\eta(z')]^2e^{-Q|z'-z_2|},\quad \eta=e,h,$$

$$C_{ij}^{\eta\vartheta}=\frac{Q_j^\eta}{Q}\int_{-\infty}^{\infty}dz'[\phi_i^\eta(z')]^2\int_{-\infty}^{\infty}dz''[\phi_j^\vartheta(z'')]^2\times e^{-Q|z'-z''|},\quad \eta,\vartheta=e,h.$$

Unlike the integral equation (A1) the linear equations (A2) can be easily solved. When the solutions x_i^η are set back into the Eq. (A1), one obtains the intercarrier interaction $V(\mathbf{Q},z_1,z_2)$ in a closed form:

$$\begin{aligned}V(\mathbf{Q},z_1,z_2)=&\frac{e}{2\kappa Q}e^{-Q|z_1-z_2|}\\&-\sum_{l=1}^{L}\frac{Q_l^e}{Q}\int_{-\infty}^{\infty}dz''[\phi_l^e(z'')]^2e^{-Q|z_1-z''|}\frac{\mathcal{D}_l(z_2)}{\mathcal{D}}\\&-\sum_{k=1}^{K}\frac{Q_k^h}{Q}\int_{-\infty}^{\infty}dz''[\phi_k^h(z'')]^2e^{-Q|z_1-z''|}\\&\times\frac{\mathcal{D}_{k+L}(z_2)}{\mathcal{D}},\end{aligned}\tag{A3}$$

where $\mathcal{D}_i/\mathcal{D}=x_i^\eta$ is the ith solution of the system (A1) [$\mathcal{D}_i$ and $\mathcal{D}$ are appropriate determinants]. The Coulomb matrix element

$$\int_{-\infty}^{\infty}dz_1\int_{-\infty}^{\infty}dz_2\phi_i(z_1)\phi_j(z_2)V(\mathbf{Q},z_1,z_2)\phi_m(z_1)\phi_n(z_2)\tag{A4}$$

is then easy to evaluate.

The e-h scattering rate (3) and the e-e scattering rate (7) are obtained using the Coulomb matrix element (A4) for $L=K=1$ and for $L=1$, $K=0$, respectively. Taking $K=0$ in the e-e interaction we neglect the screening by the holes. This corresponds to the so-called quasidynamic

approximation,[17] in which heavy holes are not able to follow the fast changes of electron positions. Finally, as in previous papers,[11,14] we restrict ourselves to the screening by quasiequilibrium carriers in the QW. In our conditions (the density of the carriers equal to 10^{11} cm^{-2} or 10^{12} cm^{-2}, the lattice temperature 8 K) the quasiequilibrium carriers occupy mainly the lowest subband of the QW. Therefore, we neglect L and K greater than 1.

[1] J. E. M. Haverkort, P. W. M. Blom, P. J. Van Hall, J. Claes, and J. H. Wolter, Phys. Status Solidi B **188**, 139 (1995).

[2] H. Shichijo, R. M. Kolbas, N. Holonyak, Jr., R. D. Dupuis, and P. D. Dapkus, Solid State Commun. **27**, 1029 (1978).

[3] J. Y. Tang, K. Hess, N. Holonyak, Jr., J. J. Coleman, and P. D. Dapkus, J. Appl. Phys. **53**, 6083 (1982).

[4] S. V. Kozyrev and A. Ya. Shik, Fiz. Tech. Poluprovodn. **19**, 1667 (1985) [Sov. Phys. Semicond. **19**, 1024 (1985)].

[5] J. A. Brum and G. Bastard, Phys. Rev. B **33**, 1420 (1986).

[6] P. W. M. Blom, C. Smit, J. E. M. Haverkort, and J. H. Wolter, Phys. Rev. B **47**, 2072 (1993).

[7] M. R. X. Barros, P. C. Becker, S. D. Morris, B. Deveaud, A. Regreny, and F. Beisser, Phys. Rev. B **47**, 10 951 (1993).

[8] A. Fujiwara, Y. Takahashi, S. Fukatsu, Y. Shiraki, and R. Ito, Phys. Rev. B **51**, 2291 (1995).

[9] K. Kálna, M. Moško, and F. M. Peeters, Appl. Phys. Lett. **68**, 117 (1996).

[10] I. Vurgaftman, Y. Lam, and J. Singh, Phys. Rev. B **50**, 14 309 (1994).

[11] P. W. M. Blom, J. E. M. Haverkort, P. J. van Hall, and J. H. Wolter, Appl. Phys. Lett. **62**, 1490 (1993).

[12] B. K. Ridley, Phys. Rev. B **50**, 1717 (1994).

[13] P. Sotirelis, P. von Allmen, and K. Hess, Phys. Rev. B **47**, 12 744 (1993).

[14] P. Sotirelis and K. Hess, Phys. Rev. B **49**, 7543 (1994).

[15] A. Mošková and M. Moško, Phys. Rev. B **49**, 7443 (1994).

[16] M. Moško and A. Mošková, Semicond. Sci. Technol. **9**, 478 (1994).

[17] M. Moško, A. Mošková, and V. Cambel, Phys. Rev. B **51**, 16 860 (1995).

[18] Ľ. Hrivnák, Appl. Phys. Lett. **56**, 2425 (1990).

[19] S. M. Goodnick and P. Lugli, Appl. Phys. Lett. **51**, 584 (1987).

[20] S. M. Goodnick and P. Lugli, in *Hot Carriers in Semiconductor Nanostructures*, edited by J. Shah (Academic, New York, 1992), p 191.

[21] A. Mošková, Ph.D. thesis, Comenius University, Bratislava, 1992.

[22] D. W. Snoke, W. W. Rühle, Y.-C. Lu, and E. Bauser, Phys. Rev. Lett. **68**, 990 (1992).

[23] M. Preisel, J. Mørk, and H. Haug, Phys. Rev. B **49**, 14 478 (1994).

[24] K. Yokoyama and K. Hess, Phys. Rev. B **33**, 5595 (1986).